IEEE Access
Multidisciplinary : Rapid Review : Open Access Journal

Received March 21, 2021, accepted March 30, 2021, date of publication April 6, 2021, date of current version April 23, 2021.

Digital Object Identifier 10.1109/ACCESS.2021.3071472

DNG Metamaterial Reflector Using SOCT Shaped Resonator for Microwave Applications

AHASANUL HOQUE[1], (Graduate Student Member, IEEE), MOHAMMAD TARIQUL ISLAM[1], (Senior Member, IEEE), ALI F. ALMUTAIRI[2], (Senior Member, IEEE), AND MUHAMMAD E. H. CHOWDHURY[3], (Senior Member, IEEE)

[1]Department of Electrical, Electronic and Systems Engineering, Faculty of Engineering and Built Environment, Universiti Kebangsaan Malaysia, Bangi 43600, Malaysia
[2]Department of Electrical Engineering, Kuwait University, Kuwait City 13060, Kuwait
[3]Department of Electrical Engineering, Qatar University, Doha, Qatar

Corresponding authors: Ahasanul Hoque (p94155@siswa.ukm.edu.my), Mohammad Tariqul Islam (tariqul@ukm.edu.my), and Ali F. Almutairi (ali.almut@ku.edu.kw)

ABSTRACT In this paper, the triple reflection band split O circled T (SOCT) shape metamaterial resonator is presented based on the transmission line principle. This paper aims to develop a miniature metamaterial resonator that can simultaneously perform as a reflector and a sensing element in the microwave range. Compare to symmetric and asymmetric structures; the reflection feature is mostly available in a typical resonating structure. The primary motivation beyond the presented work is to achieve high reflection with triple resonance points at 5.8 GHz, 6.37 GHz and 6.57 GHz. The proposed structure achieved Double Negative (DNG) features on this particular resonance with a relative permittivity value ranges -2.17 to -6.62 and relative permeability of -0.73 to -4.15. The scattering parameter performance was verified through simulation and measurement for unit cell and 5×8 array structure. An analytical sensing ability for liquid salinity was performed for potential microwave application, which indicates a potential outcome of the proposed structure in microwave sensing applications.

INDEX TERMS Reflector, metamaterial, microwave sensor, resonator, scattering parameters.

I. INTRODUCTION

Materials that have been using in electromagnetic or microwave application was explored based on dielectric characteristics. Before the last few decades, those properties were enough to meet scientific innovation's challenges until two great scientists, Sir John Pendry and Victor Veselago [1], who have set the world alight by inspiring ceaseless curiosity about ''Metamaterial''. Unlike conventional material, ''meta (beyond)-material'' describes the field of analysis of materials with negative permittivity (ε) and permeability (μ). Artificially composite material arranged in periodic structure shows negative indexed dielectric properties. This concept and experimental demonstrations by smith *et al.* [2]–[4] explored a wide range of engineered designs. Conventionally we identify the material using atomic structure or physical characteristics. The metamaterial structural unit is rationally designed to achieve negative dielectric properties and it can be customized in terms of shape, size and substrate materials. Therefore, compared to ordinary material, metamaterial properties mainly depend on geometry rather than the combination of materials. When electromagnetic (EM) waves enter a material, the electric and magnetic fields may change the material's charge distribution and induce electric and magnetic dipole moments inside the elements. A material's responses to the external EM wave radiation are macroscopically depicted by two parameters: relative dielectric permittivity ε_r and relative magnetic permeability μ_r. These two parameters characterize the collective contributions from the excited dipole moments. Usually, they do not depend on the size or the shape of the material sample, i.e., they are homogeneous and inherent properties of a material. Generally speaking, ε_{r} and μ_{r} are both positive for most ordinary materials [5]. However, in-depth analysis and state of the art design using metamaterial concept for microwave sensing is very promising [6]–[8]. Because Maxwell's equation for nanoparticle structure analysis for sensing, dielectric property at zero or negative region is quite significant.

The associate editor coordinating the review of this manuscript and approving it for publication was Santi C. Pavone.

Besides, material like graphene has spatial inhomogeneity. Optical range non-uniform conductivity shows a new direction of material development. A wide range of research scope is emerging with the metamaterial reflector based microwave sensing. Typical sensing has performance limitations in a harsh environment, which can be mitigated by introducing metamaterial reflector based microwave sensing since it has extraordinary material properties. Besides, EM Reflection in metamaterial affects the evanescent field, depending on the resonator structure. For sensing application, metamaterial reflector contributes to EM field interaction between sensing zone and material under test (MUT) through passive evanescent field modification. Thus, a typical metamaterial structure got expedite in sensing the intended scattering parameter to extract the expected sensing element. A wide of literature is also available in [9] regarding the concept, definition, and prospective metamaterial reflector applications. A similar approach was followed in most of the reported articles to explain the reflector's potentials for numerous applications.

Geometric-phase metasurface [10], [11] demonstrated that using four arbitrary wavefronts and orbital angular momentum (OAM) mode able to control circularly polarized (CP) EM wave. The potential applications of such metasurface are reconfigurable beam antenna and wireless communication. Optical range vortex beam is another widely explored metasurface configuration [12] featuring non-interleaved surface structure, integer and fractional momentum wavefront. Therefore EM wave manipulation would be possible for the wireless communication system. Furthermore, metalens performance [13] can be enhanced using the OAM so that reconfigurable antenna can be realized.

In recent years, symmetric and asymmetric shaped metamaterial resonators without reflection features are widely used in microwave sensors, such as different liquid or semiliquid dielectric characterization [14]–[16], industrial grade oil characterization [17], [18], biomedical fluid parameter estimation [19], [20]. The fundamental principle of metamaterial based microwave sensor is to sense the variation in resonance frequency and notch depth due to volume or permittivity perturbation of MUT or symmetry disruption of a resonator for differential sensing. Furthermore, different split ring resonator (SRR) with geometrical variations and lumped components exhibit polarization effect, electric and magnetic field dipole resonance. These features also enhance the sensing ability of metamaterial SRR structure in microwave range [21]–[24]. Noteworthy that, multiple ring resonator within a metamaterial structure used to achieve more resonance frequency within the operating spectrum. But the features come with a limitation of poor capacitive coupling effect and reduces the sensitivity. Besides, reported articles [25]–[27] has large geometry since resonating principle and architecture is based on size of the resonator. Therefore, prospective application field of the microwave sensors become incompatible for small scale integration.

In this paper, a balanced inner gap coupled ring with an outer single split ring resonator (SRR) based metamaterial reflector has been proposed for C band microwave sensor application. The proposed structure's inner ring has a circled T-shape that makes a balanced capacitively coupled resonating patch with an outer split O shape. Hence, the metamaterial structure named as split O circled T (SOCT) geometry. The double Negative (DNG) region in the resonator has been found in three distinct frequencies: 5.80 GHz, 6.37 GHz and 6.57 GHz with ε_r: −6.62, −3.75, −2.17 and μ_r: −1.98, −0.73, −4.15, respectively. The novelty of the manuscript is the resonating structure developed based on the transmission line principle rather than choosing a random patch structure. The reason for choosing a microstrip transmission line (TL) approach rather than a conventional split ring or complementary split ring or arbitrary parametric design method is to expedite the wave propagation mode (TEM, non-TEM) quasi-TEM) supporting. The size of the discrete lumped elements must be optimized to use multiconductor microwave circuits. A miniature structure would interact with EM waves when the lumped elements, i.e., unit cell, have reduced dimensions compared to operating wavelength. TL deals with this condition considering the characteristic impedance (Z_0) characterize by the lumped components. Hence, adopted TL would provide a closer approximation of structure and wave interaction to justify the reflection and microwave sensing principle. The TL-based principle is an essential component in modern wireless systems. It connects antennas to transmitters and receivers for impedance matching in mixers and amplifiers or as resonant elements in oscillators, reflectors, and filters. However, microwave sensing application of the unit cell reflector structure is another potentiality in a numerical environment. The analytical approach explores that the unit cell shows significant resonance shifting with the variation of seawater salinity. Numerical investigation and experiment measurement performed for unit cell and array structure. The proposed SOCT unit cell's compact geometrical shape ($0.62\lambda \times 0.62\lambda \times 0.06\lambda$) and a reflection feature highlight the potentiality of the structure.

Furthermore, the 5×8 array SOCT structure also shows a significant response to validate the reflection performance. As a part of microwave sensor potentiality, the unit cell has been simulated and measured with a dual-port SMA connection. The scattering parameter performance at this stage is quite similar to simulation. Hence, a simulated microwave sensing was executed for water salinity to observe the proposed unit cell's sensitivity. Organization of the manuscript completed as after introduction section II describe the metamaterial design approach and methodology with a subsection for dielectric characterization. Section III describe the development of design, simulation and measurement. A short description of sensing ability explains in section IV and section V summarize the manuscript.

II. METAMATERIAL REFLECTOR UNIT CELL DESIGN AND METHODOLOGY

Structural properties of metamaterial (MM) are far different compare to conventional materials properties and MM unit

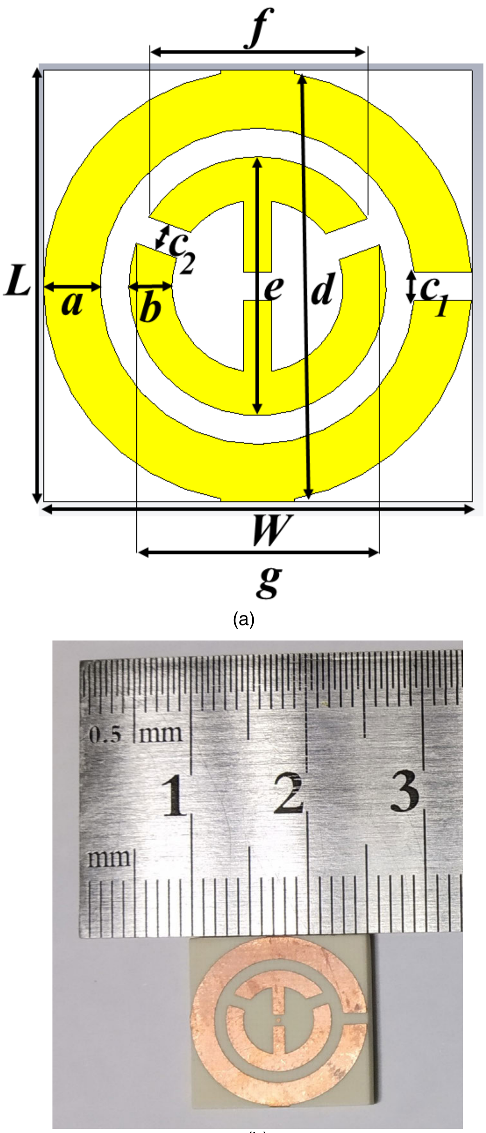

FIGURE 1. **(a) SOCT unit cell with major dimensions (b) fabricated cell.**

cell is more likely to demonstrate as an electric dipole. The proposed SOCT unit cell is shown in Figure 1(a) with major geometrical dimensions and Figure 1(b) is the fabricated one. Before explaining the design approach, a brief theoretical explanation is stated to understand the unit cell's unconventional property demonstration. Negative permittivity and permeability simultaneously demonstrate by the MM structure. The primary characterization principle of any resonator is identifying the changes in transmission (S_{21})/reflection (S_{11}) coefficients. These changes in S_{21} and S_{11} induced sensing parameter variations like dielectric value changes, permittivity, permeability, or refractive index variation. So, let's focus one by one on those parameters mathematically to extract the proposed structure effective medium characteristics. Effective medium parameter of the MM follows equation (1) for demonstrating Magnetic and Electric field rather than taking conventional field equation [14]

$$B_{ave} = \mu_{eff}\mu_0 H_{ave} \text{ and } D_{ave} = \varepsilon_{eff}\varepsilon_0 E_{ave} \tag{1}$$

where symbols have the usual meaning. Now, flux densities related to E and H field using Maxwell's equation (integral form) are

$$\int_C H.d\mathrm{I} = 0 + \frac{\partial}{\partial t}\int\int_S D.dS \text{ and } \int_C E.d\mathrm{I} = 0 - \frac{\partial}{\partial t}\int\int_S B.dS \tag{2}$$

The surface of the proposed unit cell structure calculates the integral function along the geometrical dimensions. Besides, inhomogeneous rapid variation of the magnetic field shows EM wave propagation strength through the unit cell. For homogeneous field distribution normally, permittivity becomes unity whereas equation (2) represents different distribution function of H and B. Hence, μ_{eff} become significantly altered. The dielectric properties of the proposed reflector structure extracted from conventional S-parameters response [28], [29], which led to possible uncertainties according to considered material characteristics and sample length. Moreover, the mutual effect on the complex dielectric parameters from the substrate and reflector stripline LC equivalent circuit is quite significant. The subwavelength dimension mentioned in the earlier section creates an inequality or inconsistency in spatial dispersion and therefore, we consider the weak spatial dispersion. Hence, a general idea of homogeneous field distribution for composite media and polarization-dependent metamaterial structure, we can avoid the product of wave vector (k) and dimension (d) of patch layer particle [30]. So, we can express the propagated wave as

$$\left\{\frac{\partial}{\partial x^2} + \frac{\partial}{\partial y^2} + (k^2 - \beta_z)\right\} E_z = 0 \tag{3}$$

where the z-direction is the wave propagation path, β_z is phase constant when E filed propagation is null (boundary condition). For this, the wave vector needs to satisfy, $\sqrt{k^2(\beta_x, \beta_y, 0) + \beta_z^2}$ which is contradictory for any EM wave with normal mode propagation conditions. The single ordinary EM wave has positive and negative values, which is the only possible condition when the wave vector (k) in equation (3) is second-order polynomial. Hence, dielectric properties can be extracted for an anisotropic medium using the S-parameters from the unit cell reflector. The proposed unit cell permittivity (axial component) chosen as

$$\varepsilon(k, \beta_z) = \varepsilon_h\left(1 - \frac{k_p^2}{k^2 - \beta_z^2}\right)$$

where ε_h is the permittivity of the substrate or host medium, k_p is the artificial frequency formed by patch structure and medium.

TABLE 1. SOCT unit cell dimension with major geometrical parameters.

Parameter	*L*	*W*	*a*	*b*	c_1	c_2	*d*
Size (mm)	15.0	15.00	2.01	1.50	1.00	1.01	14.77
Parameter	*e*	*f*	*g*				
Size (mm)	8.92	7.65	8.51				

However, the unit cell's subwavelength dimension is designed by Finite Integration Technique (FIT) based on commercially available CST Microwave studio software. The Rogers RO4350B substrate of 1.524 mm thickness with a 0.035 mm copper patch layer is used to realize the structure; the dielectric constant is 3.48, loss tangent is 0.0037. RO4350B is a glass microfiber reinforced PTFE composites aligned for exacting stripline and microstrip high-frequency circuit applications. The patch structure developed on top of the substrate based on Copper (Cu) (thickness 0.035mm) using standard PCB fabrication procedure. The proposed unit cell consists of two balanced ring resonators. As per the literature studied, instead of the square shape, a circular patch was chosen to avoid the bianisotropic behavior and cross-polarization effect from the metallic rings [31], [32]. The chemical etching process realizes the conductive patch pattern in the top layer and round shape ground plane. Table 1 depicts the proposed microwave reflector unit cell physical dimensions.

III. DESIGN EVOLUTION, SIMULATION AND MEASUREMENT

The gradual development of design in a sequential step followed to optimize the structure. The reflection (S_{11}) and transmission (S_{21}) parameter in dB scale has been analyzed for the design evolution. Figure 2(a,b) illustrates the performance of the parameters. It is evident that throughout the step by step process of inclusion of resonating patch, the transmission coefficient becomes more dominant rather than the reflection coefficient. For example, design-1 and design-2 separately introduce a split ring, but the scattering parameter's impact is not significant. Besides, design-3 and design-4 contribute to the individual arrangement with the outer patch, especially at the X band. Finally, combing the inner and outer split patch demonstrates a comparatively good response for S_{11} and S_{21} in magnitude (dB).

CST Microwave studio frequency-domain solver was used to perform the proposed unit cell and array structure simulation. Figure 3 shows the perspective view of the simulation setup. Both structures are placed between positive and negative Z-axis waveguide ports to excite the resonating structure. The Electric and magnetic field is placed at the X and Y axis, respectively, for creating transverse electromagnetic propagation. Reference axis used during placement of waveguide port for optimal excitation of field. Additionally, tetrahedral mesh with adaptive mesh refinement technique was adopted to perform the simulation. During free space propagation, an approximate impedance of 377Ω considered due to the substrate's dielectric characteristics.

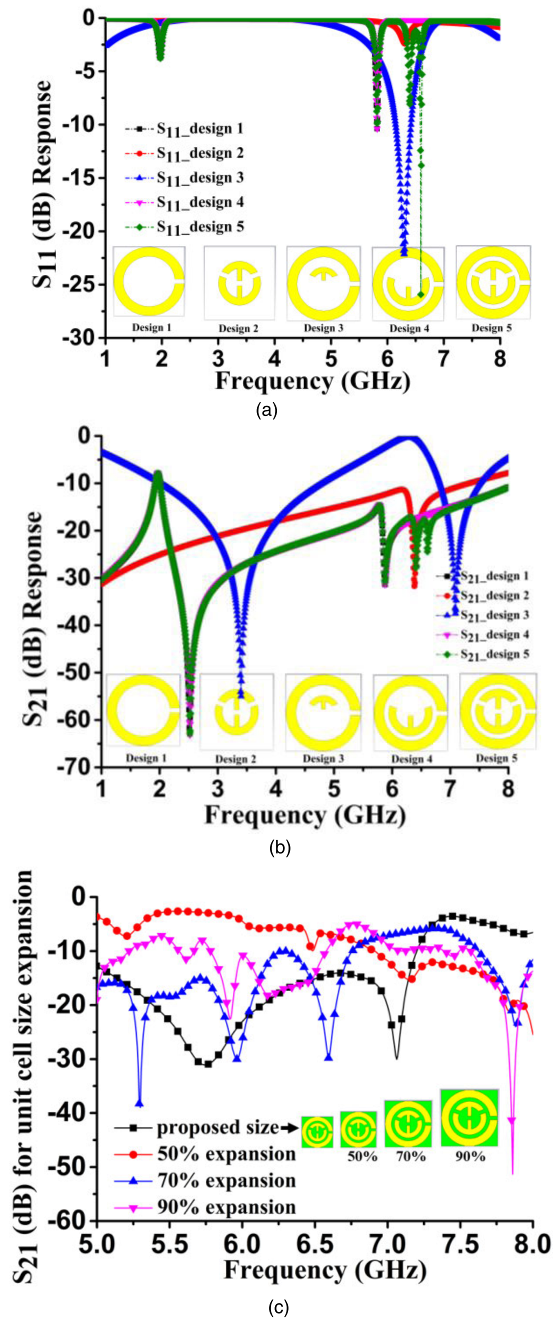

FIGURE 2. (a) Reflection (S_{11}) coefficient (b) Transmission (S_{21}) coefficient of the proposed unit cell resonator (c) Affect of unit cell size expansion on S_{21}.

After transverse mode, EM wave propagation through the unit cell, the scattering parameter from both port become available for further reflection analysis and characterization. Simulation and measurement have adopted the same characterization process: the Nicolson-Ross-Weir (NRW) method [33]. The method receives the S-parameter from the simulation or measurement facility through a vector network analyzer while placing the MUT between two waveguide ports. The details of the extraction method of NRW are available in the literature [33] and therefore proceed to

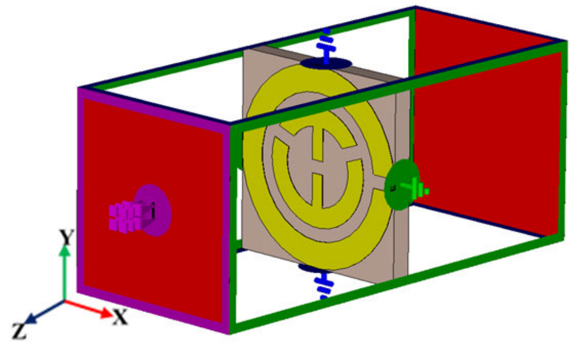

FIGURE 3. Boundary condition for the unit cell simulation.

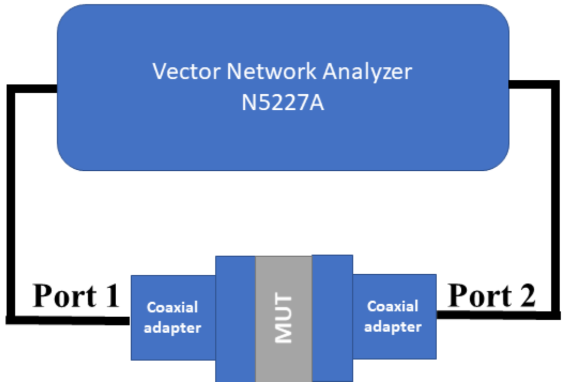

FIGURE 4. Schematic diagram of measurement set up of the proposed SOCT unit cell.

measurement steps. Figure 4 shows a schematic of the measurement setup using the PNA N5227A Microwave network analyzer. The analyzer is connected through a coaxial cable to two waveguide ports. Before starting the measurement, the analyzer is calibrated using an N4694-60001 calibration kit between 1-8 GHz.

Overall unit cell size was studied numerically from 50% to 90% extension and showed shifts in the resonance frequency (Fig. 2c). Obviously, the resonance frequency at the intended frequency band will expedite the metamaterial property deviation. The metasurface or dielectric properties of the unit cell extracted using the NRW method entirely depend on transmission and reflection parameters. Besides, the electrical wavelength of the unit cell depends on λ at the corresponding operating frequency. As the size increases, the anisotropy property also changes and affects the EM wave propagation. Hence, the unit cell is proposed with the geometrical dimension as well as array structure.

MUT is measured by placing between two waveguide ports within close contact to avoid or minimize air dielectric effect, undesired EM wave interference. Figure 4 shows the schematic diagram of waveguide port based SOCT measurement set up. A time gating function [34] from the network analyzer was used to ensure the measured signal reflected from the proposed reflector. The right-angle adapter has a dimension of 38mm × 38mm × 30 mm with a rated theoretical insertion loss of 0.25 Max. and VSWR 1.25. The guide opening dimension is 19.05mm × 9.52 mm for wave propagation. The wave passes through the waveguide port and interacts with MUT.

Parametric response shows (in simulation) triple resonance shown by the transmission and reflection coefficient as the EM wave penetrates the unit cell. Mathematical and physical explanations in this section using the spatial dispersion phenomenon would be helpful to understand. Hence, the proposed SOCT substrate stands with a multiplier, and eventually, most field components (either E-field or H-field) cannot dominate the propagation. Furthermore, the equivalent circuit model (Figure 5a) elucidates that dominating the inductive and capacitive components exists at the center and on the outer ring split gap. However, Figure 5b shows the approximation of the equivalent circuit in terms of

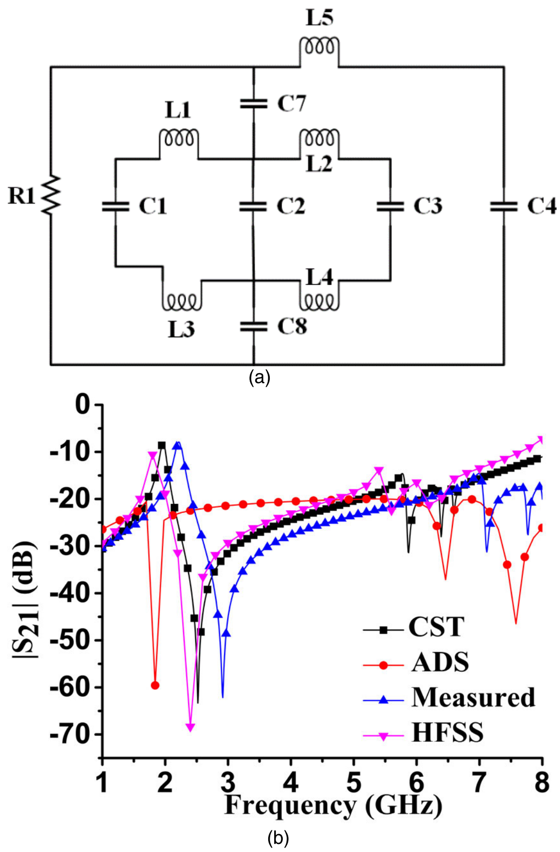

FIGURE 5. (a) Equivalent circuit model of the proposed SOCT unit cell (b) S21 response compare with CST, ADS, measured and HFSS analysis for unit cell.

transmission coefficient. The transmission line principle based circuit for the proposed SOCT unit cell RF response is quite similar compare to CST, Measured and HFSS analysis. The RF response of the circuit was evaluated using Advanced Design System (ADS) software. Thus, the exciting power and current distribution can be well approximated using the equivalent circuit model. Especially, the connected edge patch shows a strong electric field due to a steady charge carrier path (Figure 6a), and unit cell reflector inner and outer slots are responsible for consecutive other resonance

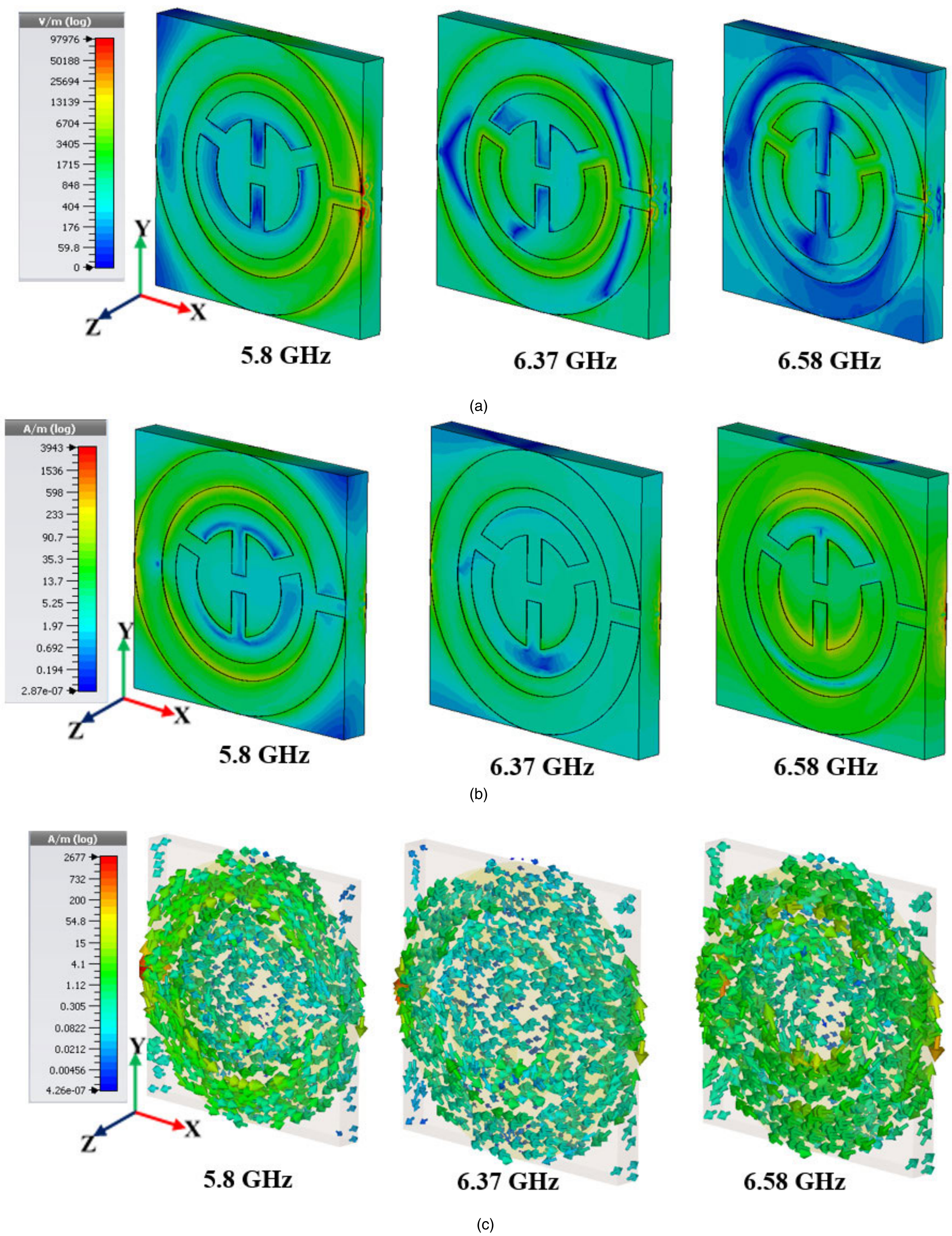

FIGURE 6. Distribution of (a) electric field (b) magnetic field (c) Surface current at three distinct resonance frequency.

frequency response regarding the fields. On the contrary, the H field (Figure 6b) at the same resonance point illustrates almost homogenous field distribution. Bianisotropic resonator structure of the proposed unit cell reflector radiates the field components following the 'Helmholtz equation,' and therefore, the field's strength gradually becomes weak. Moreover, a mutual coupling of patches moderately accepts individual fields at the center of SOCT, which accelerates resultant H-field orientation.

The surface current distribution has a significant effect shown in Figure 6c follows the transmission line component using microstrip form. Close observation in reflection (S_{11})

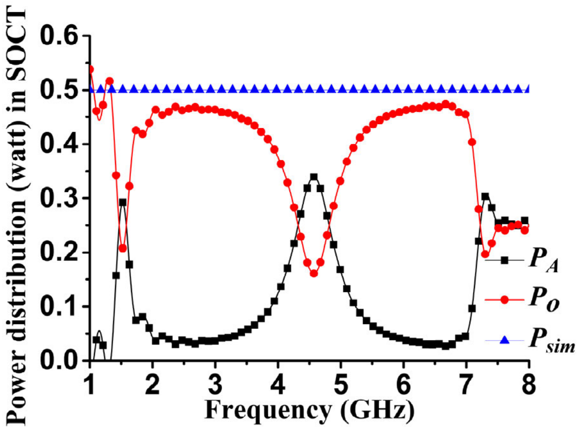

FIGURE 7. Power distribution in unit cell SOCT.

co-efficient demonstrates antisymmetric dominating current distribution at the microstrip line. Hence, an equivalent magnetic dipole moment creates a surface current loop and is responsible for the unit cell's artificial magnetism. Therefore, such a resonance is referred to as magnetic resonance, like Figure 6b.

Power loss density in the proposed absorbing unit present in Figure 7 at the same resonance frequency. The distance of power flow is dense in the transmission line region as the electric field is fed to the transmission line, and then it tends to reduce in the patch aperture area as distance increase from the feed. At the center of the unit cell feeding amount is stronger rather than a peripheral patch.

In waveguide port, amplitude, this power depends on the mode. For N excitation modes, stimulated power at the port is

$$P_s(port) = \frac{1}{2}\sum_{n=1}^{N}(A)_n^2 \tag{4}$$

where $P_s(port)$ is stimulated power at the port, and A is the amplitude of this time-harmonic excitation for ports and plane waves is constant across all frequencies (typically '1'). Hence, the proposed unit cell simulated power is 0.5W (according to simulation setup). Figure 7 depicts this stimulated power (P_{sim}) is unchanged over the frequency spectrum. Now, the real part of complex average power (P_{CA}), which is applied to the unit cell in Z-direction (positive) is given by

$$P_{CA} = \text{Re}\left\{\frac{1}{2}\int_A \vec{E}\times\vec{H}.zdz\right\} \tag{5}$$

Equation (4) is also valid for port 2 (negative Z-direction), and it describes the net energy flow into the unit cell at a specific port. By using simulated mode (TE_{11} and TM_{11}) in the proposed unit cell waveguide port, calculate for each mode, hence accepted power per port, also calculated by the software. Accepted power (P_A) and outgoing power (P_o) have identical but opposite magnitude of each other since the unit cell power concentrated more on X band rather than lower band operation.

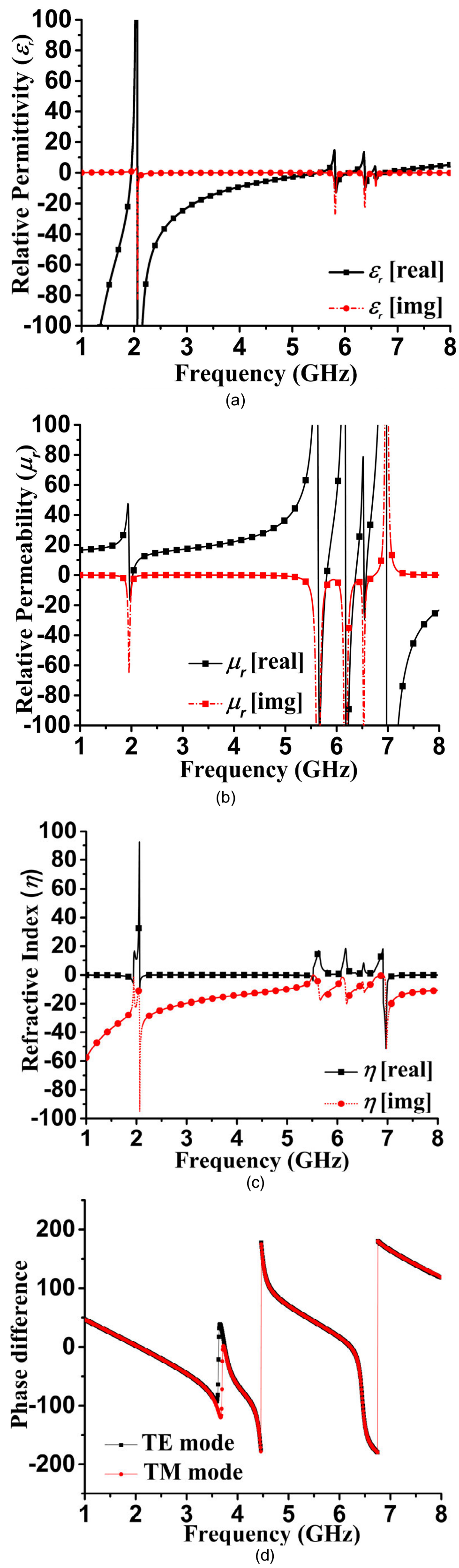

FIGURE 8. (a) Relative permittivity (b) Relative permeability (c) Refractive index using the DRI method (d) Phase variation in different EM mode (e) Polarization conversion ratio (PCR) with reflection performance.

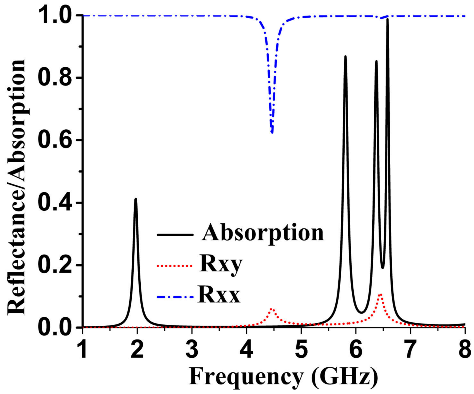

(e)

FIGURE 8. ***(Continued)*** **(a) Relative permittivity (b) Relative permeability (c) Refractive index using the DRI method (d) Phase variation in different EM mode (e) Polarization conversion ratio (PCR) with reflection performance.**

A. SOCT CHARACTERISTICS ANALYSIS

As stated earlier, boundary condition (for simulation) and waveguide port in simulation and measurement applied to extract the s parameter after EM wave propagation. The reflection (S_{11}) and the transmission (S_{21}) coefficient are scattering parameters to identify the characteristics of the unit cell concerning Electromagnetic (EM) field interactions within the targeted frequency range. Figure 2(a,b) shows transmission and reflection characteristics in the simulated spectrum. The real and imaginary part of S_{11} and S_{21} presents over X band with triple resonance point. The NRW method to calculate the refractive index [28]

$$S_{21} = js_0 S_{11} M \text{ where, } s_0 = \pm 1 \text{ and } M = \sqrt{\frac{1-|S_{11}|^2}{|S_{11}|^2}}$$

The above scattering parameter relationship depicts an unchanged magnitude with polarity change. Hence traveling EM wave in a unit cell gives no identical value despite polarization angle shifts from $-\pi$ to $+\pi$. Eventually, expecting a metamaterial property on those fluctuating points. Though the proposed SOCT unit cell demonstrates strong DNG (Double Negative) at three resonance frequencies (Figure 8a,b).

Besides, the phase difference (Figure 8d) in TE and TM mode shows a minor effect on the SOCT unit cell. But the phase difference between 5-8GHz is quite the opposite transmission signifies that a major wave variation occurs at that range. That's why the polarization conversion ratio (PCR) for E-field and H-field compared with the X and Y axis (Figure 8e). Unfortunately, the dependency on axis variation of field is quite impactful on reflection performance. On the other hand, an array of 5×8 SOCT simulated and measured to observe the s parameter performance. Though in simulation S_{21} has significant changes in resonance frequency shift but in measurement magnitude variation is relatively high due to the free space measurement error (Figure 9a-c). Further analysis of the simulated and measured data deviation found possible explanation such as-

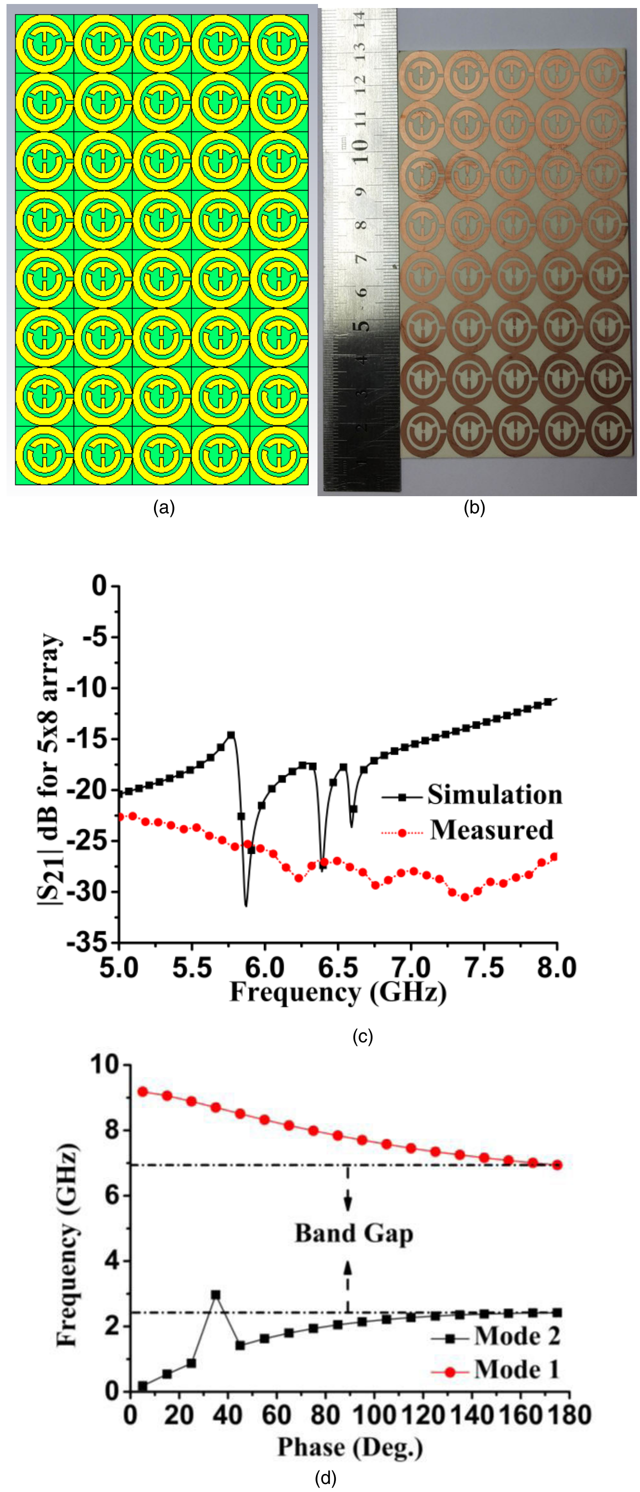

FIGURE 9. **5 × 8 array structure of the proposed SOCT resonator (a) Simulated (b) Fabricated structure (c) Simulated vs. measured S_{21} (d) Dispersion diagram of the unit cell.**

1. During measurement, the coaxial cable connecting the excitation port horn antenna and network analyzer used four (4) male to female adaptors in two 2W SMA connectors. The cable length (5m) was relatively excess due to the distance between the antenna holder (inside the

anechoic chamber) and the VNA. Therefore, the losses introduced by the impedance should be comparatively high than usual. Measured Impedance bandwidth for the array structure was gradually increasing with the transmission value. Hence, resonance frequency at the expected frequency point represented lower magnitude and shifted.

2. Before the measurement was conducted, calibration shows that reflection and transmission reference planes shifted between −10dB to −12 dB, whereas an ideal situation should be around 0dB reference plane. So, the transmission coefficient measured response shows a deviated response in terms of magnitude.

3. Array structure measurement requires proper incident angle, alignment and material position on the sample holder. The 5 × 8 array structure transmission parameter measured only line of sight (LOS) rather than a variation of angle. Therefore, the operating wavelength may become unreliable in the vicinity of 5-8 GHz and shows a discrepancy for S_{21}. However, the resonance frequency existence with shifted point represents some reflection potential in an array structure.

TE and TM mode's dispersion characteristics are already described in Fig. 8d to identify the first Brillouin Zone of the proposed unit cell structure. A similar analysis was performed during 'Eigen Mode solver' with CST Microwave Studio 2017. The solver chose the Hexahedral mesh and Jacoby Davidson Method (JDM). Two separate modes (1 and 2) were analyzed for a specific number of the structure's lowest resonance. Since only the fundamental mode is expected, the number of modes reduced to '1' and faster calculation JDM was selected. The horizontal axis in Fig. 9c represents the phase difference along Brillouin zone boundaries. The vertical axis identifies the frequency gap i.e. bandgap. The bandgap identifies the fundamental mode operation along the propagation direction. Both mode 1 and 2 tries to become equally aligned between 120 to 180(deg.) approximately. But the corresponding fundamental frequency ranges between 2.5 to 6.9 GHz i.e., bandgap 4.4 GHz for fundamental mode operation, which is a bit high. Consequently, any propagation between this bandgap would be lossy in terms of phase deviation.

IV. SENSING ANALYSIS

The proposed SOCT unit cell simulated and measured S parameter comparatively high magnitude inspired to apply the resonator in the microwave sensing application. A sharp resonance frequency with high Q factor and multiple notch at resonance is very potential for liquid sensing for sensing application. Therefore a conceptual analysis is performed in the simulation where a circular shape fluid channel crosses over the outer SRR illustrated in Figure 10a. An inlet and outlet syringe pump can be deployed to clear out the liquid after passing through the split (sensing zone in Figure 10a). Two SMA port excitation with 50Ω characteristics impedance placed between two edges of the SOCT unit resonator. During simulation, different type of water (as a liquid) passes through

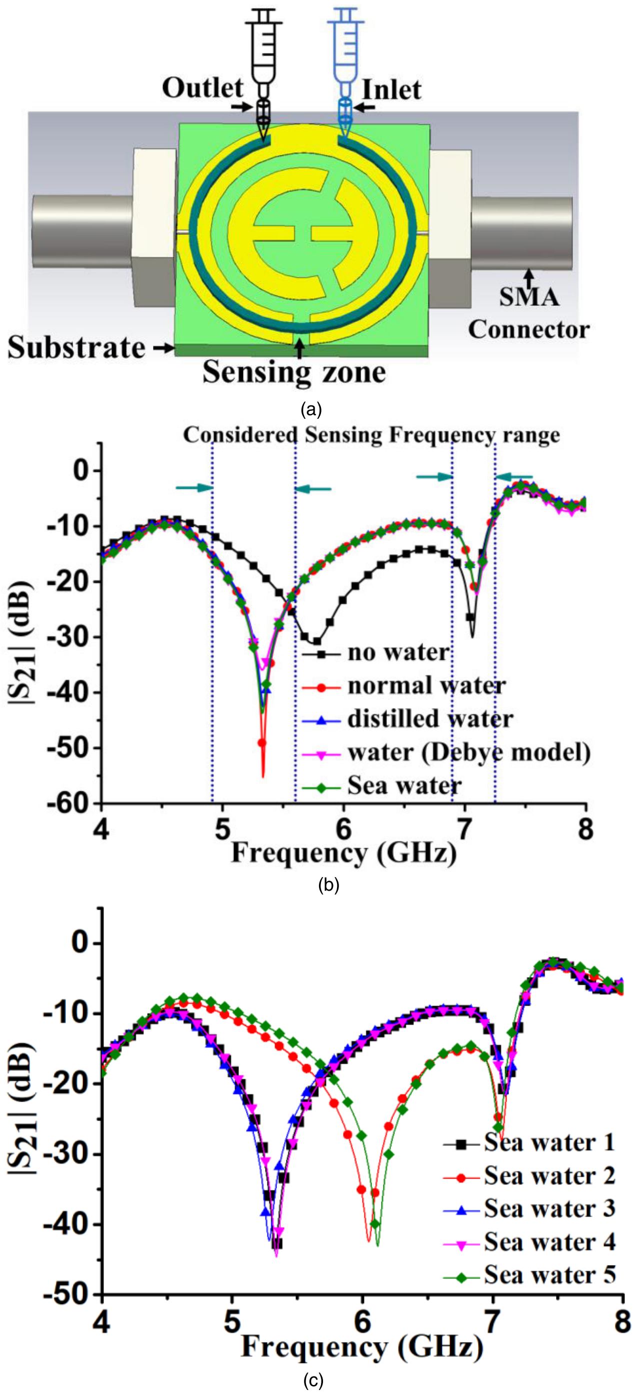

FIGURE 10. Simulation setup of the proposed SOCT resonator (a) Sensing performance analysis (b) S_{21} (dB) performance for different type of water as a liquid sensing analysis (c) S_{21} (dB) performance for salinity of seawater.

the sensing zone and among other sample seawater and normal water shows quite a good magnitude (Figure 10b). Therefore, the salinity of seawater simulated for potential impact on S_{21}. Normal seawater salinity depends on the number of factors such as geographical location, sea level, amount of nitrogen and phosphorus etc. For simplicity, the simulated seawater available in CST is taken into consideration and

TABLE 2. **Comparison between the proposed metamateial and related reflector for sensing.**

Paper	Reflection (%)	Dimension (mm)	Bandwidth	Substrate	Frequency range (GHz)	Remarks on Sensing with Reflection
[35]	Above 90	12×12	Narrow band	FR-4	C and X band	NR
[36]	Above 90	10×10	Narrow band	FR-4	X band	NR
[37]	Above 90	33 x 32	wideband	FR-4	2.7-5.7	NR
[38]	50	22.86 x 10.16	Ultra-narrow band	RT 5870	X band (8-12)	NR
[39]	Above 80	24 x 30	Narrow band	FR-4	1-6	NR
[40]	Above 80	22.86 x 10.16	wideband	FR-4	X band	NR
[41]	Above 80	10 ×10	Narrow band	SiO_2	Infrared range	NR
Proposed	Above 90	15 x 15	Fractional band	RO4350B	X band	Reflection and sensing

*NR=Not Reported

it can be changed from 50 to 90 for ε_r and corresponding conductivity ranges 3.0-3.55 S/m (Figure 10c). Hence, five (5) sample seawater varying the parameter, a numerical response of S_{21} observed on the proposed SOCT resonator. An interesting dual notch shifting in resonance frequency in samples 2-5 explains that seawater's increasing conductivity shifts the resonance to the right side. The further sample seawater experiment may demonstrate a more precise response with the proposed SOCT structure for microwave sensing.

Table 2 illustrates the proposed unit cell resonator's comparative view with other reported articles in relevant applications. Most of the authors reported absorption without sensing [31]–[36], whereas the proposed unit cell simultaneously demonstrated the reflection and sensing ability. Therefore, with further precise development and analysis, the resonator cum sensor would be a potential candidate for liquid sensing.

V. CONCLUSION

In summary, a miniature structure metamaterial resonator is proposed. The proposed structure triple fractional bandwidth reflection above 90% in simulation, whereas measured s parameter shows a quite high magnitude response. The reflector's complex structure ensures perfect metamaterial property with a minimal value of backward propagation (DNG at 5.8 GHz, at 6.37 GHz, and 6.57 GHz) for modified dielectric characteristics lead to perfect EM reflection. Besides, water salinity's sensing ability through metamaterial reflector may have other potential prospects in various commercial products in the X band. Large-area applications for remote sensing because it shows potential sensing capability to moisture content using a low-cost solution.

REFERENCES

[1] V. G. Veselago, "The electrodynamics of substances with simultaneously negative values of img align=absmiddle alt= ε Eps/Img and μ," *Physics-Uspekhi*, vol. 10, pp. 509–514, Dec. 1968.

[2] D. R. Smith, W. J. Padilla, D. C. Vier, S. C. Nemat-Nesser, and S. Schultz, "Composite medium with simultaneously negative permeability and permittivity," *Phys. Rev. Lett.*, vol. 84, p. 4184, May 2000.

[3] R. A. Shelby, D. R. Smith, S. C. Nemat-Nasser, and S. Schultz, "Microwave transmission through a two-dimensional, isotropic, left-handed metamaterial," *Appl. Phys. Lett.*, vol. 78, no. 4, pp. 489–491, Jan. 2001.

[4] R. A. Shelby, "Experimental verification of a negative index of refraction," *Science*, vol. 292, no. 5514, pp. 77–79, Apr. 2001.

[5] J. Zhu, *Design and Application of Novel Metamaterial Elements and Igurations*. London, U.K.: Oxford Univ. Press 2011.

[6] L. La Spada and L. Vegni, "Electromagnetic nanoparticles for sensing and medical diagnostic applications," *Materials*, vol. 11, no. 4, p. 603, Apr. 2018.

[7] I. Liberal and N. Engheta, "Near-zero refractive index photonics," *Nature Photon.*, vol. 11, no. 3, pp. 149–158, Mar. 2017.

[8] A. Vakil and N. Engheta, "Transformation optics using graphene," *Science*, vol. 332, no. 6035, pp. 1291–1294, Jun. 2011.

[9] S. Hannan, M. T. Islam, N. M. Sahar, K. Mat, M. E. H. Chowdhury, and H. Rmili, "Modified-segmented split-ring based polarization and angle-insensitive multi-band metamaterial absorber for X, Ku and K band applications," *IEEE Access*, vol. 8, pp. 144051–144063, 2020.

[10] Y. Yuan, K. Zhang, B. Ratni, Q. Song, X. Ding, Q. Wu, S. N. Burokur, and P. Genevet, "Independent phase modulation for quadruplex polarization channels enabled by chirality-assisted geometric-phase metasurfaces," *Nature Commun.*, vol. 11, no. 1, pp. 1–9, Dec. 2020.

[11] Y. Yuan, S. Sun, Y. Chen, K. Zhang, X. Ding, B. Ratni, Q. Wu, S. N. Burokur, and C. Qiu, "A fully phase-modulated metasurface as an energy-controllable circular polarization router," *Adv. Sci.*, vol. 7, no. 18, Sep. 2020, Art. no. 2001437.

[12] K. Zhang, Y. Yuan, X. Ding, H. Li, B. Ratni, Q. Wu, J. Liu, S. N. Burokur, and J. Tan, "Polarization-engineered noninterleaved metasurface for integer and fractional orbital angular momentum multiplexing," *Laser Photon. Rev.*, vol. 15, no. 1, Jan. 2021, Art. no. 2000351.

[13] K. Zhang, Y. Yuan, X. Ding, B. Ratni, S. N. Burokur, and Q. Wu, "High-efficiency metalenses with switchable functionalities in microwave region," *ACS Appl. Mater. Interface*, vol. 11, no. 31, pp. 28423–28430, Aug. 2019.

[14] M. Saadat-Safa, V. Nayyeri, M. Khanjarian, M. Soleimani, and O. M. Ramahi, "A CSRR-based sensor for full characterization of magneto-dielectric materials," *IEEE Trans. Microw. Theory Techn.*, vol. 67, no. 2, pp. 806–814, Feb. 2019.

[15] X. Zhang, C. Ruan, T. U. Haq, and K. Chen, "High-sensitivity microwave sensor for liquid characterization using a complementary circular spiral resonator," *Sensors*, vol. 19, p. 787, Feb. 2019.

[16] E. L. Chuma, Y. Iano, G. Fontgalland, and L. L. B. Roger, "Microwave sensor for liquid dielectric characterization based on metamaterial complementary split ring resonator," *IEEE Sensors J.*, vol. 18, no. 24, pp. 9978–9983, Mar. 2018.

[17] N. Kumar Tiwari, S. Prakash Singh, and M. Jaleel Akhtar, "Novel improved sensitivity planar microwave probe for adulteration detection in edible oils," *IEEE Microw. Wireless Compon. Lett.*, vol. 29, no. 2, pp. 164–166, Feb. 2019.

[18] L. Su, J. Mata-Contreras, P. Vélez, A. Fernández-Prieto, and F. Martín, "Analytical method to estimate the complex permittivity of oil Samples," *Sensors*, vol. 18, no. 4, p. 984, 2018.

[19] M. T. Islam, A. Hoque, A. F. Almutairi, and N. Amin, "Left-handed metamaterial-inspired unit cell for S-band glucose sensing application," *Sensors*, vol. 19, no. 1, p. 169, Jan. 2019.

[20] N. Alrayes and M. I. Hussein, "Metamaterial-based sensor design using split ring resonator and Hilbert fractal for biomedical application," *Sens. Bio-Sens. Res.*, vol. 31, Feb. 2021, Art. no. 100395.

[21] A. Salleh, C. Yang, T. Alam, M. Singh, M. Samsuzzaman, and M. Islam, "Development of microwave brain stroke imaging system using multiple antipodal vivaldi antennas based on raspberry Pi technology," *J. Kejuruteran*, vol. 32, pp. 1–6, Feb. 2020.
[22] J. D. Baena, J. Bonache, F. Martin, R. M. Sillero, F. Falcone, T. Lopetegi, M. A. G. Laso, J. Garcia-Garcia, I. Gil, M. F. Portillo, and M. Sorolla, "Equivalent-circuit models for split-ring resonators and complementary split-ring resonators coupled to planar transmission lines," *IEEE Trans. Microw. Theory Techn.*, vol. 53, no. 4, pp. 1451–1461, Apr. 2005.
[23] J. Bonache, M. Gil, I. Gil, J. Garcia-Garcia, and F. Martin, "On the electrical characteristics of complementary metamaterial resonators," *IEEE Microw. Wireless Compon. Lett.*, vol. 16, no. 10, pp. 543–545, Oct. 2006.
[24] M. A. H. Ansari, A. K. Jha, and M. J. Akhtar, "Design and application of the CSRR-based planar sensor for noninvasive measurement of complex permittivity," *IEEE Sensors J.*, vol. 15, no. 12, pp. 7181–7189, Dec. 2015.
[25] T. Haq, C. Ruan, S. Ullah, and A. Kosar Fahad, "Dual notch microwave sensors based on complementary metamaterial resonators," *IEEE Access*, vol. 7, pp. 153489–153498, 2019.
[26] K. Zhang, R. K. Amineh, Z. Dong, and D. Nadler, "Microwave sensing of water quality," *IEEE Access*, vol. 7, pp. 69481–69493, 2019.
[27] L. Su, J. Mata-Contreras, P. Velez, and F. Martin, "Splitter/combiner microstrip sections loaded with pairs of complementary split ring resonators (CSRRs): Modeling and optimization for differential sensing applications," *IEEE Trans. Microw. Theory Techn.*, vol. 64, no. 12, pp. 4362–4370, Dec. 2016.
[28] A. Hoque, M. Tariqul Islam, A. Almutairi, T. Alam, M. Jit Singh, and N. Amin, "A polarization independent quasi-TEM metamaterial absorber for X and Ku band sensing applications," *Sensors*, vol. 18, no. 12, p. 4209, Nov. 2018.
[29] D. R. Smith, S. Schultz, P. Markoá, and C. M. Soukoulis, "Determination of effective permittivity and permeability of metamaterials from reflection and transmission coefficients," *Phys. Rev. B, Condens. Matter*, vol. 65, no. 19, Apr. 2002, Art. no. 195104.
[30] F. Capolino, *Theory and Phenomena of Metamaterials*. Boca Raton, FL, USA: CRC Press, 2017.
[31] R. Marques, F. Mesa, J. Martel, and F. Medina, "Comparative analysis of edge- and broadside-coupled split ring resonators for metamaterial design–Theory and experiments," *IEEE Trans. Antennas Propag.*, vol. 51, no. 10, pp. 2572–2581, Oct. 2003.
[32] S. I. Maslovski, P. M. T. Ikonen, I. Kolmakov, S. A. Tretyakov, and M. Kaunisto, "Artificial magnetic materials based on the new magnetic particle: Metasolenoid," *Prog. Electromagn. Res.*, vol. 54, pp. 61–81, 2005.
[33] E. J. Rothwell, J. L. Frasch, S. M. Ellison, P. Chahal, and R. O. Ouedraogo, "Analysis of the nicolson-ross-weir method for characterizing the electromagnetic properties of engineered materials," *Prog. Electromagn. Res.*, vol. 157, pp. 31–47, 2016.
[34] R. Parashkov, E. Becker, T. Riedl, H.-H. Johannes, and W. Kowalsky, "Large area electronics using printing methods," *Proc. IEEE*, vol. 93, no. 7, pp. 1321–1329, Jul. 2005.
[35] M. Agarwal, A. K. Behera, and M. K. Meshram, "Closed ring resonator based absorber for C and X band applications," in *Proc. IEEE Appl. Electromagn. Conf. (AEMC)*, Dec. 2015, pp. 1–2.
[36] M. Hossain, M. Faruque, M. Islam, and K. Mat, "A new compact octagonal shape perfect metamaterial absorber for microwave applications," *Appl. Sci.*, vol. 7, no. 12, p. 1263, Dec. 2017.
[37] K. Ling, M. Yoo, and S. Lim, "Frequency tunable metamaterial absorber using hygroscopicity of nature cork," *IEEE Antennas Wireless Propag. Lett.*, vol. 14, pp. 1598–1601, 2015.
[38] M. Bakir, M. Karaaslan, O. Akgol, O. Altintas, E. Unal, and C. Sabah, "Sensory applications of resonator based metamaterial absorber," *Optik*, vol. 168, pp. 741–746, Sep. 2018.
[39] M. Bakär, M. Karaaslan, F. Dincer, K. Delihacioglu, and C. Sabah, "Tunable perfect metamaterial absorber and sensor applications," *J. Mater. Sci., Mater. Electron.*, vol. 27, no. 11, pp. 12091–12099, Nov. 2016.
[40] Y. I. Abdulkarim, L. Deng, O. Altintaş, E. Ünal, and M. Karaaslan, "Metamaterial absorber sensor design by incorporating swastika shaped resonator to determination of the liquid chemicals depending on electrical characteristics," *Phys. E, Low-dimensional Syst. Nanostruct.*, vol. 114, Oct. 2019, Art. no. 113593.
[41] B. Slovick, Z. G. Yu, M. Berding, and S. Krishnamurthy, "Perfect dielectric-metamaterial reflector," *Phys. Rev. B, Condens. Matter*, vol. 88, no. 16, Oct. 2013, Art. no. 165116.

AHASANUL HOQUE (Graduate Student Member, IEEE) received the B.Sc. degree in electrical and electronic engineering (EEE) from the Chittagong University of Engineering and Technology (CUET), Chittagong, Bangladesh, in 2008, and the M.Sc. degree in electrical engineering from Karlstad University, Sweden, in 2012, with a specialization in microwave communication and signal processing. He is currently pursuing the Ph.D. degree with Universiti Kebangsaan Malaysia (UKM). He has been an Assistant Professor with the Department of Electrical and Electronics Engineering, International Islamic University Chittagong, since 2015. He has authored or coauthored a number of refereed journals and conference papers. His research interests include meta-material absorber, microwave engineering, wireless communication, solar energy harvesting, and meta-material.

MOHAMMAD TARIQUL ISLAM (Senior Member, IEEE) is currently a Professor with the Department of Electrical, Electronic and Systems Engineering, Universiti Kebangsaan Malaysia (UKM) and a Visiting Professor with the Kyushu Institute of Technology, Japan. He has supervised about 30 Ph.D. theses, 20 M.Sc. theses, and has mentored more than ten postdoctorals and visiting Scholars. He is the author and coauthor of about 500 research journal articles, nearly 200 conference papers, and a few book chapters on various topics related to antennas, metamaterials, and microwave imaging with 22 inventory patents filed. Thus far, his publications have been cited 7200 times and his H-index is 41 (Source: Scopus). His Google scholar citation is 10 700 and H-index is 48. His research interests include communication antenna design, metamaterial, satellite antennas, and microwave imaging. He was served as an Executive Committee Member for IEEE AP/MTT/EMC Malaysia Chapter, from 2019 to 2020, the Chartered Professional Engineer (CEng), a Fellow of IET, U.K., and a Senior Member of IEICE, Japan. He received several International Gold Medal Awards, a Best Invention in Telecommunication Award for his Research and Innovation, and the Best Researcher Awards from UKM. He was a recipient of more than 40 research grants from the Malaysian Ministry of Science, Technology and Innovation, Ministry of Education, UKM Research Grant, and International Research Grants from Japan, Saudi Arabia, and Kuwait, the 2018, 2019, and 2020 IEEE AP/MTT/EMC Malaysia Chapter, Excellent Award, the Publication Award from Malaysian Space Agency, in several years, the Best Innovation Award, and the Best Research Group in ICT niche from UKM, in different years. He was an Associate Editor of *IET Electronics Letters*. He also serves as the Guest Editor for *Sensors* journal and an Associate Editor for IEEE ACCESS.

ALI F. ALMUTAIRI (Senior Member, IEEE) received the B.S. degree in electrical engineering from the University of South Florida, Tampa, FL, USA, in 1993, and the M.S. and Ph.D. degrees in electrical engineering from the University of Florida, Gainesville, FL, USA, in 1995 and 2000, respectively. In December 1993, he has been awarded a full scholarship from Kuwait University to pursue his graduate studies. From March 2007 to September 2011, he was the Chairperson of the Department of Electrical Engineering, Kuwait University. From September 2015 to September 2016, he was the Graduate Program Director of the Department of Electrical Engineering, Kuwait University. From March 2016 to July 2018, he was the Vice Dean of Academic Affairs, College of Engineering and Petroleum, Kuwait University. From July 2018 to December 2020, he was the Dean of Admission and Registration, Kuwait University. He is currently a Professor with the Department of Electrical Engineering. His current research interests include multiuser detection, wireless networks, antenna design, and current and future cellular networks performance issues. He is a member of other professional societies. He served/serving as an associate editor and a reviewer for many technical publications.

MUHAMMAD E. H. CHOWDHURY (Senior Member, IEEE) received the B.Sc. and M.Sc. degrees (Hons.) from the Department of Electrical and Electronics Engineering, University of Dhaka, Bangladesh, and the Ph.D. degree from the University of Nottingham, U.K., in 2014. He worked as a Postdoctoral Research Fellow and a Hermes Fellow with the Sir Peter Mansfield Imaging Centre, University of Nottingham. Before joining Qatar University, he worked with several universities in Bangladesh. He is currently working as a full-time Faculty Member with the Department of Electrical Engineering, Qatar University. He is also running several NPRP and UREP grants from QNRF and internal grants from Qatar University along with academic and government projects. He has been involved in EPSRC, ISIF, and EPSRCACC grants along with different national and international projects. He has worked as a Consultant for the projects entitled, Driver Distraction Management Using Sensor Data Cloud from 2013 to 2014, the Information Society Innovation Fund (ISIF), Asia. He has a patent and published around 60 peer-reviewed journal articles, conference papers, and two book chapters. His current research interests include biomedical instrumentation, signal processing, wearable sensors, medical image analysis, machine learning, embedded system design, and simultaneous EEG/fMRI. He is an Active Member of British Radiology, Institute of Physics, ISMRM, and HBM. He received the ISIF Asia Community Choice Award 2013 for a project entitled Design and Development of Precision Agriculture Information System for Bangladesh. He has recently won the COVID-19 Dataset Award for his contribution to fight against COVID-19. He is serving as an Associate Editor for IEEE Access and a Review Editor for *Frontiers in Neuroscience*.